EXPLICIT FIBER BEAM-COLUMN ELEMENTS FOR IMPACT ANALYSIS OF STRUCTURES

Samer Sabry F. Mehanny Gendy [(1)], Ashraf Ayoub [(2)]

[1] Ph.D. Candidate, School of Mathematics, Computer Science & Engineering, Department of Civil Engineering; City, University of London, London, UK; E-mail: Samer.Gendy@city.ac.uk

[2] (corresponding author) Professor, School of Mathematics, Computer Science & Engineering, Department of Civil Engineering; City, University of London, London, UK; E-mail: Ashraf.Ayoub.1@city.ac.uk

Abstract

The solution of impact problems requires advanced computational techniques to overcome the difficulties associated with large short-duration loads. In this case, the explicit time integration method is typically used, since it provides a stable solution for problems such as the analysis of structures subjected to shock and impact loads. However, most explicit-based finite elements were developed for continuum models such as membrane and solid elements, which renders the problem computationally expensive. On the other hand, the development of fiber-based beam finite elements allows for the simulation of the global structural behavior with very few degrees of freedoms, while accounting for the detailed material nonlinearity along the element length. However, explicit-based fiber beam elements have not been properly formulated, in particular for the case of the emerging force-based beam element.

In this paper, two developed fiber plane beam elements that consider an explicit time integration scheme for the solution of the dynamic equation of motion are presented. The first element uses a displacement-based formulation, while the second element uses a force-based formulation. For the latter case, a new algorithm that eliminates the need for iterations at the element level is proposed. The developed elements require the use of a lumped mass matrix and a small time increment to ensure numerical stability. No iterations or convergence checks

are required, which renders the problem numerically efficient. The developed explicit fiber beam-column models, particularly the force-based element, represents a simple yet powerful tool for simulating the nonlinear complex effect of impact loads on structures accurately while using very few finite elements. The traditional implicit method of analysis typically fails to provide numerical stable behavior for such short time duration problems.

Two correlation studies are presented to highlight the efficiency of the developed elements in modelling impact problems where the strain rate effect is considered in the material models. These examples confirm the accuracy and efficiency of the presented elements.

KEY WORDS

Explicit analysis, fiber beam modelling, drop weight impact test, force-based element, displacement-based element.

INTRODUCTION

The fiber beam element is known to be an advanced and numerically efficient element for the analysis of nonlinear dynamic problems **(Spacone et al. 1996, Neuenhofer and Filippou 1997, Mullapudi and Ayoub 2010)**. However, the existing fiber beam elements use an implicit time integration method that requires a large number of iterations per time step to reach convergence. In several dynamic analyses, particularly for impact and blast problems, the solution cannot be achieved due to severe numerical difficulties **(Bathe and Cimento 1980 and Yang et al. 1995)**.

Meanwhile, commercial finite element software programs are widely used to model impact problems using the explicit algorithm. However, most of the elements used for these types of analysis are continuum-based elements. **Huang and Wu (2009)** studied the dynamic impact of a vertical concrete cask tip-over using the explicit capability in the software LS-DYNA. **Hong et al. (2014)** created a numerical model to simulate the response of non-composite steel-concrete-steel sandwich panels under impact loading using the same software. Recently, **Chen et al. (2016)** simulated the effect of a large-size truck hitting a reinforced concrete column using also LS-DYNA. In all these studies, solid elements were used to simulate the impact problems. These models required considerable execution time, large storage memory, and slow post-processing. On the other hand, the fiber plane beam element requires much less storage size, smaller execution time, and fast post-processing.

Moreover, several researchers used the explicit time integration technique to solve different structural problems under dynamic loading. **Kujawski (1988)** presented a semi-explicit algorithms for dynamic non-linear problems using iteratively only forward substitution that allows the utilization of both consistent and lumped mass matrix. **Miranda et al. (1989)** derived an explicit predictor-corrector algorithm from the implicit alpha-method. It was found that the explicit algorithm has a better stability and higher accuracy when compared with a Newmark-based predecessor. The algorithm is utilized for the solution of linear and non-linear structural dynamics problems. **Pezeshk and Camp (1995)** developed an explicit time integration technique for dynamic analyses of linear undamped single degree of freedom systems. The technique was based on a modified trapezoidal rule to approximate the governing ordinary differential equation. It was found that the new explicit procedure is more accurate in determining the transient response with the same amount of computational cost when compared with the modified Euler method procedure.

Sun et al. (2000) compared the performance of an implicit and explicit finite element methods for two dynamic problems (an elastic bar and a cylindrical disk on a rigid wall) using the ABAQUS finite element software. For the fast linear contact problems, it was found that the advantages of the explicit method are apparent within a desirable tolerance.

Chang (2009) presented a new explicit method with enhanced stability. The new explicit method have unconditional stability for general instantaneous stiffness hardening systems in addition to linear elastic and instantaneous stiffness softening systems, where the instantaneous stiffness is a parameter used by the author to describe the variation of stiffness for a non-linear system. It was found that the new method is efficient for the solution of a general structural dynamic problems where the response is dominated by low-frequency modes and when high frequency responses are of no interest. The method was also found to be second-order accurate.

Fulei and Yungui (2011) used the finite rotation theory to determine the node direction vectors and the Yoshida method **(Yoshida et al. 1980)** to find the element direction vectors of a nonlinear beam element. The authors formulated their element in a corotational system and used an explicit algorithm for the solution of nonlinear dynamic structures. The authors compared their results with the ANSYS explicit commercial software.

Lately, **Tenek (2015)** presented a three-dimensional explicit beam finite element with the derivation of an initial load due to temperature. The element was employed to analyse beams, arches, and frame structures.

Many of the previously published work concentrated on employing simple material models. However, the accurate prediction of the complex structural response requires more rigorous material models able to depict the performance of the structure under severe loading conditions. In this study, two explicit fiber beam elements are formulated. The presented

elements use advanced nonlinear material models for both concrete and steel members for the accurate representation of nonlinear behaviour along the element length. The developed elements are implemented in the research-oriented finite element analysis program FEAP developed by **Taylor (2014)**.

EXPLICIT AND IMPLICIT TIME INTEGRATION METHODS

Explicit dynamic analysis is a mathematical method for integrating the equations of motion through time. The explicit procedure is suitable for high-speed short time duration analysis as stated by **Gu and Wu (2013)**. It is conditionally stable, which means that a small time increment has to be used to ensure that the solution is stable. So, longer analysis runtime should be expected in the explicit analysis.

In the explicit analysis, dynamic values for the current step are obtained from values already known from the previous step by solving for time $(t + \Delta t)$ using values from the preceding time(t), where (t) is the time elapsed and (Δt) is the time increment as shown in Fig. (1). Also no convergence check is needed as the nodal accelerations are calculated directly by multiplying the inverse of the mass matrix by the force vector.

However, in the implicit method, values for the next step are obtained from values from both the current step and the later one by solving for time $(t + \Delta t)$ using data from time (t) and $(t + \Delta t)$. Thus a Newton-Raphson iteration technique is essential to find the solution and to enforce equilibrium by iterating until convergence is achieved.

Therefore, the explicit method is conditionally stable with no required convergence checks, necessitates many relatively inexpensive time steps, and is suitable for short transient dynamic problems. On the other hand, the implicit method is unconditionally stable and

entails convergence checks at all times, requires small number of expensive time steps, and is typically suitable for static and quasi static problems. In general, the implicit method can lead to convergence problems as it is more sensitive to initial conditions and non-linear behavior.

STABILITY OF THE EXPLICIT METHOD

The explicit method gives accurate solution as long as the numerical stability is maintained, which is known as a conditionally stable method. Therefore a small time step is required for explicit analysis and the time step should be assessed before attempting the solution. In this process, the chosen time increment (Δt) must be less than the stable time increment(Δt_{min}).

The stable time increment is calculated by:

$$\Delta \mathrm{t}_{min} = \frac{L}{c_d} \tag{1}$$

where c_d is the dilatational wave speed, $c_d = \sqrt{\frac{E}{\rho}}$ (2)

E is the material Young's modulus, ρ is the material density and L is the element length. Decreasing L or increasing c_d will reduce the stable time increment.

DYNAMIC FORMULATION OF THE EXPLICIT METHOD

The dynamic equilibrium equation of motion that describes the motion of a body subjected to a force can be generally written in the following form:

$$M\ddot{U}_t + C\dot{U}_t + KU_t = F_t \tag{3}$$

Where M is the mass matrix and K is the stiffness matrix, F_t is the vector of external forces and $M\ddot{U}_t$ represents the inertia force while $C\dot{U}_t$ represents the damping force.

The damping matrix C can be determined using the Rayleigh damping equation:

$$C = \alpha_m M + \beta_k K \quad (4)$$

Where α_m is the mass proportional Rayleigh damping parameter and β_k is the stiffness proportional Rayleigh damping parameter. They are calculated based on the natural frequencies of the first modes and their damping ratios. The solution of the dynamic equation of motion for the developed beam elements is conducted in the corotational reference frame as described next.

COROTATIONAL FORMULATION OF THE DEVELOPED FIBER BEAM ELEMENTS

The presented elements are formulated in the corotational frame where the rigid body modes are removed before the dynamic effect is added in the global frame. The corotational element has three natural degrees of freedom, an axial elongation e and two rotations θ_1 and θ_2 at each end of the element. The axial force P and the moments M_1 and M_2 at both ends are the corresponding element nodal forces and are shown in Fig. (2). The global frame consists of six degrees of freedom (four translations and two rotations) and six corresponding forces. Next, the explicit formulations used in this paper are discussed in details.

EXPLICIT FORMULATION OF THE DISPLACEMENT-BASED ELEMENT

In the first explicit fiber beam element a displacement-based formulation is used where equilibrium is satisfied in a weighted integral sense.

The internal and external forces, ($F_{internal}$ and $F_{external}$) respectively, are summed at each node point, and the nodal accelerations are computed by multiplying the forces with the inverse of the nodal mass:

$$[M]\{\ddot{U}\}_t = [F_{external}]_t - [F_{internal}]_t \quad (5)$$

The explicit algorithm uses the Newmark beta-gamma method with the primary variables being displacement increments to calculate the displacement, velocity and acceleration. Accordingly, the solution to Equation (3) leads to the following:

$$U_{t+1} = U_t + \Delta t\dot{U}_t + \frac{1}{2}(1-\beta)\Delta t^2\ddot{U}_t + \frac{1}{2}\beta\Delta t^2\ddot{U}_{t+1} \quad (6)$$

$$\dot{U}_{t+1} = \dot{U}_t + (1-\gamma)\Delta t\ddot{U}_t + \gamma\Delta t\ddot{U}_{t+1} \quad (7)$$

$$M\ddot{U}_{t+1} + C\dot{U}_{t+1} + KU_{t+1} - F_{t+1} = 0 \quad (8)$$

For an implicit solution, $\beta = 0.25$ and $\gamma = 0.5$, while the explicit algorithm assume $\beta = 0$ and $\gamma = 0.5$, then calculate the acceleration $\ddot{U}_t$ at time (t) by making use of the inversion of the mass matrix based on equation (5), followed by calculating the displacement U_{t+1} using equation (6). The evaluation of the mass matrix is described in detail in a subsequent section. The velocity $\dot{U}_{t+1}$ and the acceleration $\ddot{U}_{t+1}$ are then calculated explicitly at time (t+1) by using the two equations (7) and (8).

The algorithm starts by assuming an *Explicit Parameter* to equal 1 for explicit dynamic analysis.

The equivalent global dynamic stiffness $\hat{K}_{elem(global)}$ is substituted by the lumped mass matrix:

$$\hat{K}^{t+1}_{elem(global)} = Explicit\ Parameter\ \times\ M \quad (9)$$

And the global internal dynamic load $\hat{F}_{elem(global)}$ is determined as:

$$\hat{F}^{t+1}_{elem(global)} = F^{t+1}_{elem(global)} + M\ \ddot{U}^{t+1} + (\alpha_m M + \beta_k K)\dot{U}^{t+1} \quad (10)$$

where $F_{elem(global)}$ is the static element load vector in the global frame. This is calculated through integration of sections along the element length and discretization of each section

into fibers with prescribed nonlinear material behaviour. The global element force increment is:

$$\Delta\hat{F}_{elem(global)}^{t+1} = \hat{F}_{external}^{t+1} - \hat{F}_{elem(global)}^{t+1} \tag{11}$$

Where $\hat{F}_{external}$ is the applied external force corresponding to the load step.

Then at the global level, the finite element solution for an acceleration increment in the global frame $\Delta\ddot{U}_{(global)}$ is computed by:

$$\Delta\ddot{U}_{(global)}^{t+1} = \left[\hat{k}_{elem(global)}^{t+1}\right]^{-1} \times \Delta\hat{F}_{elem(global)}^{t+1} \tag{12}$$

In the explicit solution, ΔU is then calculated from $\Delta\ddot{U}_{(global)}$ using equations (6 to 8) as detailed before.

The evaluation of the stiffness matrix K_{elem} and load vector F_{elem} is first calculated in the corotational frame, then transformed to the global frame by adding the rigid body modes as follows:

$$k_{elem(global)}^{t+1} = T^T\, K_{elem}^{t+1}\, T \tag{13}$$

$$F_{elem(global)}^{t+1} = T^T\, F_{elem}^{t+1} \tag{14}$$

Where T is the transformation matrix $= \begin{bmatrix} -1 & 0 & 0 & 1 & 0 & 0 \\ 0 & \frac{1}{L} & 1 & 0 & -\frac{1}{L} & 0 \\ 0 & \frac{1}{L} & 0 & 0 & -\frac{1}{L} & 1 \end{bmatrix}$ (15)

To determine the value of K_{elem} and F_{elem} using the displacement-based method in the corotational frame, the section deformation increment of the element reference axis in the corotational frame is first evaluated as:

$$d_s^{t+1} = S\, \Delta q^{t+1} \tag{16}$$

Where S is the displacement shape function = $\begin{bmatrix} \frac{1}{L} & 0 & 0 \\ 0 & \frac{-4}{L}+\frac{6\,x}{L} & \frac{-2}{L}+\frac{6\,x}{L} \end{bmatrix}$ (17)

The calculation of the displacement increment Δq in the corotational frame is accomplished using the matrix T:

$$\Delta q^{t+1} = T\,\Delta U^{t+1} \tag{18}$$

The element stiffness can then be calculated as:

$$K_{elem}^{t+1} = \int_0^L S^T\, k_{sec}^{t+1}\, S\, dx \tag{19}$$

Where k_{sec} is the section stiffness. And the element internal resisting force vector is equal to:

$$F_{elem}^{t+1} = \int_0^L S^T\, F_{sec}^{t+1}\; dx \tag{20}$$

Where F_{sec} is the section resisting forces in the corotational frame.

$$F_{sec}^{t+1} = \begin{Bmatrix} p \\ M \end{Bmatrix} \tag{21}$$

Where p is the section axial force and M is the section bending moment.

The section stiffness k_{sec} and force vector F_{sec} are determined from fiber discretization as noted earlier using the section deformation increment and following the assumption of plane sections remaining planes:

$$\varepsilon_1\,(x,y) = \varepsilon(x) - y\,\emptyset(x) \tag{22}$$

Where ε_1 is the fiber axial strain, ε is the axial strain at the beam axis, y is the distance from the neutral axis, and $\emptyset$ is the section curvature. The fiber strain is used along with the fiber nonlinear material constitutive law to determine the fiber force and stiffness, which are integrated along the section depth to evaluate the section force and stiffness.

The second order analysis is considered into the formulations by adding the geometric stiffness matrix **(Alemdar and white 2005)**.

Concisely to consider the second order effect, the stiffness matrix must be updated by adding the internal geometric stiffness matrix term K_g:

$$K_{elem}^{t+1} = \left(K_g^{t+1} + \int_0^L N_\delta^T \, k_{sec}^{t+1} \, N_\delta dx\right) \tag{23}$$

$$\text{Where } K_g^{t+1} = P^{t+1} \begin{bmatrix} \frac{2L}{15} & \frac{-L}{30} & 0 \\ \frac{-L}{30} & \frac{2L}{15} & 0 \\ 0 & 0 & 0 \end{bmatrix} \tag{24}$$

And P is the axial force in the corotational frame.

Therefore equation (19) is replaced by equation (23) and the resisting load vector is evaluated by:

$$F_{elem}^{t+1} = \int_0^L N_\delta^T \, F_{sec}^{t+1} \, dx \tag{25}$$

Where $N_\delta =$

$$\begin{bmatrix} \frac{1}{L} & (1-4x+3x^2)^2\theta_1 + & (1-4x+3x^2)(-2x+3x^2)\theta_1 + \\ & (1-4x+3x^2)(-2x+3x^2)\theta_2 & (2x+3x^2)^2\theta_2 \\ 0 & -\frac{4}{L}+\frac{6x}{L} & -\frac{2}{L}+\frac{6x}{L} \end{bmatrix} \tag{26}$$

So equation (20) is substituted by equation (25).

EXPLICIT FORMULATION OF THE FORCE-BASED ELEMENT

In the second explicit fiber beam element, a force-based formulation is used where the equilibrium is satisfied in a section by section basis along the element length. In the newly proposed algorithm, normal internal iterations are avoided and the solution procedure is only

conducted once to calculate the element stiffness matrix and load vector. The use of this technique is accurate as long as the time step is set to be smaller than a critical value. However, if adopting a time step larger than the critical value, performing internal iterations would be needed to minimize the internal residual error. In this case, the solution is transformed into a mixed explicit implicit approach.

Equations (5 to 8) are used to calculate the global acceleration, velocity and displacement explicitly at time (t+1). The dynamic stiffness $\widehat{K}_{elem(global)}$ and the dynamic load $\widehat{F}_{elem(global)}$ are then evaluated using equations (9 & 10).

Here K_{elem} and F_{elem} are determined using a force-based procedure in the corotational reference frame.

The same matrix T described in equation (15) is used to transform the system to a corotational frame. Δq^{t+1} is again evaluated using equation (18).

First the element initial end force increments are calculated with the use of the stiffness of the element at the previous step:

$$\Delta F_{elem}^{t+1} = K_{elem}^{t}\, \Delta q^{t+1} \tag{27}$$

Then the new element end forces F_{elem}^{t+1} are updated by ΔF_{elem}^{t+1}:

$$F_{elem}^{t+1} = F_{elem}^{t} + \Delta F_{elem}^{t+1} \tag{28}$$

Where $(t+1)$ denotes the new increment step and (t) denotes the previous step as the external load is imposed in an incremental sequence.

Using the force interpolation function, the section force increments ΔF_{sec} are determined by:

$$\Delta F_{sec}^{t+1} = b\, \Delta \mathrm{F}_{elem}^{t+1} \tag{29}$$

Where b is the force interpolation function and can be expressed as = $\begin{bmatrix} 1 & 0 & 0 \\ 0 & 1-x & x \end{bmatrix}$ (30)

The total section forces $F_{sec}(x)^{t+1}$ are calculated by adding the section force increments ΔF_{sec}^{t+1} to the previous section forces $F_{sec}^{t}(x)$:

$$F_{sec}^{t+1}(x) = F_{sec}^{t}(x) + \Delta F_{sec}^{t+1} \quad (31)$$

The section deformation increments are at that point established by the linearization of the section force-deformation and then used to update the section deformation d_{sec}^{t}.

$$d_{sec}^{t+1} = d_{sec}^{t} + f_{sec}^{t+1}\, \Delta F_{sec}^{t+1} \quad (32)$$

Where f_{sec}^{t+1} is the section flexibility calculated from the fibers.

To avoid violating the equilibrium, the section unbalanced forces are considered; which are the difference between the calculated total section forces and the section resisting forces. The section resisting forces are evaluated from discretization of the section into fibers using the updated section deformation d_{sec}^{t+1} and following the assumption of plane sections remaining planes:

$$F_{U}^{t+1}(x) = F_{sec}^{t+1}(x) - F_{R}^{t+1}(x) \quad (33)$$

Where F_U is the section unbalance force vector, and F_R is the resisting force vector. And thereafter the unbalanced forces are converted to a residual section deformation *r(x)* using the current section flexibility:

$$r^{t+1}(x) = f_{sec}^{t+1}\, F_{U}^{t+1}(x) \quad (34)$$

The residual element deformations is then calculated by integrating the residual section deformations along the element length:

$$R^{t+1} = \int_0^l b^T(x)\, r^{t+1}(x)\, dx \quad (35)$$

To insure numerical stability of the force based element, the residual *R* has to be minimized to a very small acceptable value. In the implicit force-based algorithm, an element iteration is needed in order to eliminate the section residual deformation r. This is performed using the following energy criteria:

$$\sum_1^3 F_{\ unbalanced} \cdot \Delta q \ \leq \ absolute\ tolerance \tag{36}$$

Where $F_{\ unbalanced}$ is the difference between the applied force and the resisting force.

In the explicit algorithm, a similar approach could be used, which requires an element-level iteration until convergence is achieved. However, the element iteration becomes unnecessary if the analysis time step is sufficiently small to satisfy the previous energy condition.

In this case, $(\sum_1^3 F_{\ unbalanced} \cdot \Delta q\ )$ is compared to the '$absolute\ tolerance$' for each element; and if found smaller this means that the element converges with one iteration only. If found larger, however, the algorithm calculates a new critical time step $\Delta t_{critical}$:

$$\Delta t_{critical}{}^{new} = \Delta t_{critical}{}^{old} \times \sqrt{\frac{absolute\ tolerance}{\sum_1^3 F_{\ unbalanced} \cdot \Delta q}} \tag{37}$$

Where the tolerance value is typically varied between 10^{-4} to 10^{-8} depending on the problem being analysed and the accuracy desired by the user.

Finally, the chosen $\Delta t_{critical}$ is the minimum $\Delta t_{critical}$ of all elements. Hence, the time step is reduced to equal $\Delta t_{critical}$.

Therefore in addition to the condition of the stable time increment Δt_{min}, if the time step is smaller than or equal to $\Delta t_{critical}$, a single iteration is sufficient to satisfy the element-level convergence criteria described in (37), and the entire solution algorithm would not require any iterations.

Once the element residual deformations are reduced to within the specified tolerance value, the element end resisting forces are updated and the element flexibility f_{elem} is estimated by the integration of the section flexibility f_{sec} along the element length. Then the element stiffness K_{elem} is computed by inverting the flexibility of the element.

$$(K_{elem}^{t+1})^{-1} = f_{elem}^{t+1} = \int_0^L b^T f_{sec}^{t+1} b \, dx \tag{38}$$

And as a last step, the forces and deformations of all sections are updated using the new element end resisting forces.

A flowchart diagram summarizing the algorithm of the proposed explicit fiber beam elements is shown in Fig. (3).

COMPUTATION OF THE MASS MATRIX

The formulation of the developed elements requires that a mass matrix be constructed. A diagonal mass matrix based on direct lumping should be used to make the inversion of the mass matrix trivial. All diagonal terms of the lumped mass matrix have to be defined, as shown in Fig. (4), including a rotational mass.

To evaluate the mass matrix due to self-weight of a beam with element length L, cross section area A and a uniform mass density ρ:

The translational nodal masses in both horizontal and vertical directions = $\frac{1}{2} \rho AL$ (39)

The rotational mass at each node = $\alpha \rho A L^3$ (40)

Where from **Felippa (2013)** the value of α varies between 0 and 1/100. If the α value is taken as zero this lead to a singular mass matrix, which cannot be used in an explicit formulation. However, higher values of α might stabilize the system without scarifying its accuracy.

For the presented elements, the value of α was taken equal to $(3.5/100)$ and was found to yield stable and accurate results for the displacement and the force based explicit elements. Whereas, for the implicit analysis, the value of α can be taken equal to zero.

In addition, external masses supported by the element can be lumped at the element ends.

CONCRETE AND STEEL MATERIAL MODELS

The concrete uniaxial material model used by the fiber beam element is based on the **Kent and Park (1971)** constitutive law as extended by **Scott et al. (1982),** while considering the strain rate effect (Fig.5). The stress-strain curve of concrete captures the nonlinear relation between the stress and strain and takes into account the effect of the confinement of concrete, the hysteretic behavior under cyclic loading and the effect of tension stiffening. The reinforcing steel model adopted by the fiber beam element is based on the **Menegotto and Pinto (1973)** constitutive law, as modified by **Filippou et al. (1983)** to account for isotropic hardening. The model considers the Bauschinger effect and the strain hardening effect as shown in Fig. (6). In the proposed element, strain rate effects are also accounted for in the material models.

To consider the strain rate effect in the material models, the material parameters of the concrete and steel were modified using the dynamic amplification factor (DAF). The DAF is a non-dimensional parameter and is used to present the difference between the properties of the materials under static and dynamic loading. The DAF can be applied to the concrete and steel material parameters to reflect the strain rate effect.

For the concrete, the value of the concrete compressive strength, the concrete strain at maximum strength and the concrete tensile strength are amplified, and for the steel reinforcement the value of the yield strength is increased.

The following equations retrieved from the literature were used in the material model. For normal concrete, the dynamic compressive strength was determined by **Fujikake et al. (2009)**:

$$f'_{cd} = f'_c \left(\frac{\dot{\varepsilon}}{\dot{\varepsilon}_s}\right)^{0.006[\log \dot{\varepsilon}/\dot{\varepsilon}_{st}]^{1.05}} \quad for\ \dot{\varepsilon} \geq \dot{\varepsilon}_{sc} \tag{41}$$

And the strain corresponding to the dynamic compressive strength was calculated as:

$$\varepsilon'_{cd} = \varepsilon'_c \left(\frac{\dot{\varepsilon}}{\dot{\varepsilon}_s}\right)^{-0.036+0.01\log(\dot{\varepsilon}/\dot{\varepsilon}_{st})} \quad for\ \dot{\varepsilon}\ \geq \dot{\varepsilon}_{sc} \tag{42}$$

Where:

f'_{cd} = The dynamic concrete compressive strength at strain rate $\dot{\varepsilon}$ in MPa.

f'_c = The static compressive strength in MPa.

ε'_{cd} = The dynamic strain corresponding to f'_{cd}.

ε'_c = The static strain corresponding to f'_c.

$\dot{\varepsilon}_{sc} = 1.2 \times 10^{-5}$.

For the dynamic tensile strength of normal concrete, the **Ross et al. (1989)** equation was used:

$$f_{td} = f_t \exp\left[0.00126\left(\log_{10}\frac{\dot{\varepsilon}}{\dot{\varepsilon}_{st}}\right)^{3.373}\right] \quad for\ \dot{\varepsilon} \geq\ \dot{\varepsilon}_{st} \tag{43}$$

Where:

f_{td} = The dynamic concrete tensile strength at strain rate $\dot{\varepsilon}$.

f_t = The static concrete tensile strength.

$\dot{\varepsilon}_{st} = 1.0 \times 10^{-7}$.

To consider the effect of fiber reinforced concrete on the DAF, the **Lok and Zhao (2004)** equations were employed. They used the Split Hopkinson pressure bar in the development of the strain rate tests that ranged between 20 and 100 s^{-1} and proposed two equations to express the compressive response of steel fiber-reinforced concrete subjected to different strain rates as follow:

$$DAF = 1.080 + 0.017\ \log(\dot{\varepsilon})\ \ 0 \le \dot{\varepsilon} \le 20\ S^{-1} \tag{44}$$

$$DAF = 0.067 + 0.796\ \log(\dot{\varepsilon})\quad 20 \le \dot{\varepsilon} \le 100\ S^{-1} \tag{45}$$

For the reinforcing steel, and according to **Limberger et al. (1982)** and **Ammann et al. (1982)** the steel elastic modulus E_S and the strain hardening modulus E_{SP} are not affected by the loading rates. So in the steel material model, only the effect on the yield strength is considered. The dynamic yield strength f_{syd} at strain rate $\dot{\varepsilon}$ is estimated by the **Malvar (1998)** equations. **Malvar (1998)** studied the strength enhancement of steel reinforcing bars under the effect of high strain rates and proposed a formula to approximate the straight line on the logarithmic scale of the dynamic increase factor versus the strain rate.

The equations were derived and are valid for a yield stress f_y that ranges between 290 and 710 MPa and are as follows:

$$DAF = \left(\frac{\dot{\varepsilon}}{10^{-4}}\right)^{\gamma} \tag{46}$$

For yield stress calculation: $\gamma = \alpha_{fy}$; $\alpha_{fy} = 0.074 - 0.04\left(f_y/414\right)$ (47)

For ultimate stress calculation: $\gamma = \alpha_{fu}$; $\alpha_{fu} = 0.019 - 0.009\left(f_y/414\right)$ (48)

Where:

$\dot{\varepsilon}$: The strain rate is in s^{-1}.

f_y : The bar yield strength in MPa.

VALIDATION OF THE NUMERICAL MODEL FOR IMPACT PROBLEMS

Instrumented drop weight tests are widely used to evaluate the response of reinforced concrete members under impact loads. **Hrynyk and Vecchio (2014)** used a drop-weight machine to test intermediate-scale slabs under impact loading. **Saatci and Vecchio (2009)** tested several reinforced concrete beams using the drop weight test and validated their numerical model. **Fujikake et al. (2009)** also used the same method to impact reinforced concrete beams and compared their results with analytical methods.

In this research, two experiments from the literature are used to validate the developed fiber beam finite elements that use the explicit time integration method. In the selected experiments, instrumented drop weight impact tests were used to examine the dynamic behavior of doubly reinforced concrete beams and steel fiber-reinforced concrete beams.

- First experiment: Impact Behavior of Reinforced Concrete Beams

An instrumented experimental program was carried out by **Saatci and Vecchio (2009)** where eight reinforced concrete beam specimens were tested under free-falling drop-weights. All the specimens had a section of 250 mm x 410 mm and a total length of 4880 mm. The beams were simply supported with a clear span of 3000 mm. All the specimens were doubly reinforced with equal top and bottom reinforcement that consist of 4 bars with diameter 29.9 mm and a yield stress of 464 MPa. Fig. (7) illustrates the impact test setup used in the experiment.

For specimen SS3a-1, the drop-weights impacted the specimen once at the mid span, from a clear height of 3.26 m, with a small drop weight (211 kg). A flexural failure mode was observed for this sample under the static loading with visible wide vertical flexural cracks at

the mid span. However, shear cracks also developed under the impact test mainly after other multiple impacts.

Specimen SS3a-1 was chosen to be modelled with the fiber beam elements. The Specimen had a compressive strength of 46.7 MPa and a strain at peak compressive strength equal to 2.51×10^{-3}. The strain rate effect in this sample was small and didn't change the material properties much. Fig. (8) displays the impact force and the reaction forces obtained from the experiment. In the finite element models, each element was divided into 5 sections and the sections were further divided into 12 concrete fibers and 4 steel fibers (Fig. 9).

A convergence study is first performed for the explicit displacement-based element. The beam was modelled with 10, 14, 18 and 22 elements including the cantilever parts. Fig. (10) shows that 18 explicit-based elements were sufficient to reach convergence.

So for the displacement based elements, the beam was subdivided into 18 finite elements. Regarding the displacement based implicit element a step of 0.01 was adopted while for the displacement based explicit element a step of 0.01 was unstable and a smaller step of 0.001was used. The impact load was applied in the middle of the beam under force control and the displacement time history was compared with the experimental results.

Similarly, for the force based elements, the beam was divided into 12 elements to reach convergence. The same time steps used with the displacement based element were also used.

Fig. (11) shows the midpoint displacement vs time response retrieved from the explicit and implicit displacement and force based elements. Both four elements produced similar results. Good agreement can be seen for both, the impact and free vibration phases.

The displacement based implicit element performed on average 4 global iterations in every step to reach convergence. While the force based implicit element performed on average 2 internal iterations and 4 global iterations in every step to reach convergence.

For the fully explicit force based element, the element is initially assigned a large time step of 0.01 and the behavior of the element was monitored as follow:

First it was found that the element was facing stability problems from an early stage. For the solution for time steps between 0 and 0.04 sec, the largest $\sum_1^3 F_{\ unbalanced} \cdot \Delta q$ ranged between (1.30E-06 and 2.74E-05) and element residual deformations R ranged between 0.3E-7 and 0.6E-5. For the largest value of $\sum_1^3 F_{\ unbalanced} \cdot \Delta q = 2.74E-05$, using Equation (37) and assuming a tolerance value of $1.00E-05$:

$\Delta t_{critical}^{\ new} = 0.01 \times \sqrt{\frac{1.00E-05}{2.74E-05}} = 0.00604\ sec$ (which is the minimum $\Delta t_{critical}$ of the 12 elements). This new time step was used in the analysis to avoid internal element iterations.

For the rest of the time steps, $\sum_1^3 F_{\ unbalanced} \cdot \Delta q$ ranged between (-0.23E-05 and 0.10E-02):

$\Delta t_{critical}^{\ new} = 0.01 \times \sqrt{\frac{1.00E-05}{0.10E-02}} = 0.001$ sec

Using the new time step 0.001, the element didn't perform any internal iterations and the element residual deformations R ranged between 0.10E-30 and 0.10E-10, satisfying convergence.

Table 1 shows the execution time each element used to solve the problem and the size of the main output file. From the table, it can be observed that because implicit elements use larger time step they require less execution time (about one fifth of that of explicit elements in this

case), and smaller output files. The elimination of the iterations did not save time as the selected time step played the major role in determining the execution time. Further, the explicit force based element required a smaller execution time than the explicit displacement based element mainly because a coarse mesh was adopted. This experiment confirmed the ability of the explicit elements in modelling the impact behavior of reinforced concrete beams while avoiding internal and external element iterations.

Table 1. Comparison between execution time of the implicit and the explicit displacement and force based elements for sample SS3a-1.

Element type	**Displacement based**		**Force based**	
	Implicit	**Explicit**	**Implicit**	**Explicit**
Time step	0.01	0.001	0.01	0.001
Elements mesh size	18	18	12	12
Execution time (mn:sec)	00:28.8	02:16.5	00:23.9	01:50.6
Main output file size (MB)	6.83	13.40	6.62	13.39

- Second experiment: Impact response of reinforced concrete beam

Fujikake et al. (2009) tested several reinforced concrete (RC) beams under impact loadings using a drop hammer impact test. Fig. (12) shows the drop hammer impact test setup used in the experiment. The beams were designed to allow for an overall flexural failure. The authors also used an analytical model that consists of a two-degree-of-freedom mass-spring-damper system to simulate the RC beams analytically. The system consisted of one degree of freedom to express the local impact response between the drop weight and the beam and

another one to express the overall response of the beam. The analysis technique involved the determination of the moment-curvature relationship of the beam using section by section analysis procedure whereas the strain rate effects were considered. Then the calculation of the load-midspan deflection relationship using the moment-curvature relationship was performed.

The two Specimens S1616-A and S1616-D were chosen to be modelled with the fiber beam elements. The RC beam specimens had a rectangular cross section of 250x150 mm and a total span length of 1400 mm. The beams were simply supported at their ends and were allowed to freely rotate while preventing them from moving out of plane. The beams were reinforced with 2Ø16 top and bottom bars with yield strengths of 426 MPa. The concrete compressive strength was 42 MPa.

The impact forces applied in the middle of the beams retrieved from the experiment are shown in Fig. (13) for sample S1616-A and Fig. (14) for sample S1616-D. Both the implicit and explicit fiber beam elements were used to simulate the behavior of the two beams under the impact force. Due to symmetry, only half of the beams were modelled with a variable number of elements. The beam in this problem was assumed simply-supported, which allows for free rotation at the ends while preventing vertical displacements; and symmetry was respected in the middle by allowing vertical movement and preventing horizontal movement and rotations. Consequently no second order effect is expected in this case.

Each element was divided into five sections and each section was further divided into 12 concrete fibers and 4 steel fibers that represent the top and bottom reinforcement (Fig. 15).

The drop hammer used had a mass of 400 kg and was dropped freely onto the top surface of the RC beam at the mid span from different heights. For specimen S1616-A, the drop height

was the smallest with 0.15m and for specimen S1616-D the drop height was the highest with 1.2m.

A laser displacement sensor was used to measure the midspan deflection of the beam and a dynamic load cell was utilized to measure the contact force between the hammer and the beam.

Specimen S1616-A

The impact force time history was used as input for the two fiber beam elements. This was retrieved from the experiment. In the implicit model, the step size was chosen as 0.001 sec and an excessive maximum of 20 iterations per step was allowed (although usually 4 to 8 iterations are commonly sufficient). The total number of steps was 2500. In the explicit force-based model, the time step size was chosen as 0.00001 to satisfy Δt_{min} and $\Delta \mathrm{t}_{critical}$ based on a fully explicit element with no iteration and a required tolerance of $1.00\mathrm{E}-06$, thus 250000 steps were used.

For the proposed criteria of the force based explicit model, the element was first assigned a large time step of 0.001, and the behavior of the element is monitored below:

The element worked well at the initial stage between steps 0 and 0.544 sec, $\sum_1^3 F_{\ unbalanced} \cdot \Delta \mathrm{q}$ ranged between (0.12E-46 and 0.83E-30) and the element residual deformations R ranged between 0.2E-14 and 0.7E-29.

Then from steps 0.544 to 1.23 sec, the largest $\sum_1^3 F_{\ unbalanced} \cdot \Delta \mathrm{q}$ ranged between (0.95E-05and 0.43E-10) and element residual deformations R ranged between 0.29E-06 and 0.95E-11).

For the largest value of $\sum_1^3 F_{\ unbalanced} \cdot \Delta q = 1.26E-06$ and, using equation (37) with a tolerance value of $1.00E-06$, $\Delta t_{critical}{}^{new} = 0.001 \times \sqrt{\frac{1.00E-06}{0.95E-05}} = 0.00032\ sec.$ This new time step ensured no element iterations are performed.

Later, between time steps 1.23 sec and the end of the analysis, $\sum_1^3 F_{\ unbalanced} \cdot \Delta q$ ranged between (0.50E-02 and 0.44E-07)

Thus $\Delta t_{critical}{}^{new} = 0.001 \times \sqrt{\frac{1.00E-06}{0.50E-02}} = 0.000014$ sec

Using a new time step of 0.000014 sec, the element didn't perform any internal iterations and R ranged between 0.10E-30 and 0.10E-16.

For the explicit displacement-based model, the time step size was chosen as 0.0001 to fulfil the Δt_{min} requirement. A diagonal lumped mass was adopted for the explicit analysis.

The material constitutive parameters used in the finite element model considering the strain rate effect were taken as follow:

$f'_{cd} = 52$ MPa, $\varepsilon'_{cd} = 0.009$, $f_{td} = 3$ MPa and $f_{syd} = 580.0\ MPa$.

With only two elements, the two explicit models were able to follow the input load-time curve and to predict the displacement-time history accurately as shown in Fig. (16). On the other hand, both of the implicit models, the displacement and force elements, suffered from severe convergence issues and resulted in unstable behavior and inaccurate displacement estimates (Fig. 16). It is worth mentioning that both explicit elements converged with only two elements as the impact load was small for this specimen. Fig. (17) shows the bending moment distribution along the span of beam S1616-A at the maximum displacement using the explicit force based element. Due to the assumption of the force-based formulation, the bending moment is linear within each element.

The difference between the capabilities of the explicit and implicit elements is very clear in this problem, which emphasises the superiority of the explicit time integration methods for short time duration impact problems. It should be noted that the explicit force-based element requires a higher number of time steps in case no internal element iterations is allowed when compared with the mixed explicit implicit force-based element or the explicit displacement-based element.

Specimen S1616-D

For the implicit model, the step size was also chosen as 0.001 and the total number of steps was 3500. In the explicit force-based model, the time step size was initially chosen as 0.00001 based on a fully explicit element with no iteration at all and a tolerance of $1.00\mathrm{E}-06$, thus 350000 steps were used. For the explicit displacement-based model, the time step size was chosen the same as the one used to solve specimen S1616-A. A diagonal lumped mass was created for the explicit element.

For the material parameters, the values considering the strain rate effect were taken as follow: $f'_{cd} = 44.0$ MPa, $\varepsilon'_{cd} = 0.0950$, $f_{td} = 1.0$ MPa and $f_{syd} = 430.0\ MPa$.

As seen in Fig. (18), only the two explicit models were able to predict the behavior of the impact problem to a good extent with four elements for the force-based and eight elements for the displacement-based approach. Both of the implicit models, the displacement and force elements, failed to follow the input path and produced exaggerated deflection values. The two fiber beam elements overcome the complexity of the analysis method used by **Fujikake et al. (2009).** Further, the force-based explicit element produced better results than the displacement-based explicit element as it requires less number of elements to reach convergence (Fig. 18). Fig.19 shows the bending moment along the span of beam S1616-D at

the maximum displacement using the explicit force based element. It also confirms the linear distribution of the moment function.

The ability of the implicit element to solve short term dynamic problems is limited and is due to several factors including the impact force value, the load input path complication, the duration of the load and the nonlinear material behavior. On the other hand, the use of explicit techniques with the fiber beam element is an advanced method to solve highly nonlinear dynamic problems without the need for iterations and convergence complications. The elements benefit from their simplicity which makes them competitive with complex continuum elements available in commercial finite element software.

CONCLUSION

In this paper, two plane fiber beam elements are presented that adopt an explicit time integration scheme to solve short-term dynamic problems, particularly impact problems where a high force is applied over a very short duration. The elements can be used reliably to analyse different reinforced concrete structures to ensure their safety against impact loading.

The elements use a displacement-based and a force-based formulation respectively, and benefit from advanced material models that can simulate the nonlinear behavior of concrete and steel materials. The developed elements overcome the difficulties and complications that are accompanied with the implicit time integration method, such as the need to iterate in every time step and the convergence requirements. Yet, the explicit element necessitates the use of a diagonal lumped mass matrix and the chosen time increment has to be smaller than the stable time increment required to maintain the stability of the numerical solution. Additionally for the fully explicit force-based element, a single iteration can be used if another critical time step is respected. The developed explicit fiber beam-column models,

particularly the force-based element, represent a simple yet powerful tool for analysis of complex impact problems efficiently while using a limited number of finite elements.

The results of the two plane elements were compared with experimental tests of impact problems in order to validate their accuracy, and promising outcomes were obtained.

Future work will attempt to expand the current formulation to the three-dimensional space including second order and shear deformation effects. Analysis under blast loads will be evaluated.

REFERENCES

Alemdar, B. and White, D. (2005). "Displacement, Flexibility, and Mixed Beam–Column Finite Element Formulations for Distributed Plasticity Analysis." *J. Struct. Eng.*, 131(12), pp.1811-1819.

Ammann, W., Muehlematter, M., & Bachmann, H. (1982). "Stress-strain behaviour of non prestressed and prestressed reinforcing steel at high strain rates." *Proc. of RILEM-CEB-IABSE-IASS*, Concrete structures under impact and impulsive loading, p. 656, Berlin, BAM

Bathe, K. and Cimento, A. (1980). "Some practical procedures for the solution of nonlinear finite element equations." Computer Methods in Applied Mechanics and Engineering, 22(1), pp.59-85.

Chang, S. (2009). "An explicit method with improved stability property." *International Journal for Numerical Methods in Engineering*, 77(8), pp.1100-1120.

Chen, L., Xiao, Y., and El-Tawil, S. (2016). "Impact Tests of Model RC Columns by an Equivalent Truck Frame." *J. Struct. Eng.*, 10.1061/(ASCE)ST.1943-541X.0001449, 04016002.

Felippa, C. (2013). "*Matrix Finite Element Methods in Dynamics (Course in Preparation)*." 1st ed. [ebook] Colorado, Chapter 18. <http://www.colorado.edu/engineering/CAS/courses.d/MFEMD.d/MFEMD.Ch18.d/MFEMD.Ch18.pdf> (Dec. 6, 2016).

Filippou, F.C., Popov, E.P., and Bertero, V.V. (1983). "Effects of Bond Deterioration on Hysteretic Behavior of Reinforced Concrete Joints." Report No. UCB/EERC-83/19, Earthquake Engineering Research Center, University of California, Berkeley, p. 191.

Fujikake, K., Li, B. and Soeun, S. (2009). "Impact Response of Reinforced Concrete Beam and Its Analytical Evaluation." *Journal of Structural Engineering*, 135(8), pp. 938-950.

Fulei, W. and Yungui, L. (2011). "A Nonlinear Dynamic Beam Element with Explicit Algorithms." *Communications in Computer and Information Scienc*, CCIS 163, pp. 311-318.

Gu, L. and Wu, S. (2013). "Introduction to the explicit finite element method for nonlinear transient dynamics". Hoboken, N.J.: Wiley, p.5.

Hong, S.G., Lee, S.J. and Lee, M.J. (2014). "Steel plate concrete walls for containment structures in Korea: in-plane shear behavior." *Infrastruct Syst Nucl Energy*, pp. 237–257

Hrynyk, T. and Vecchio, F. (2014). "Behavior of Steel Fiber-Reinforced Concrete Slabs under Impact Load." *ACI Structural Journal*, 111(5).

Huang, C. and Wu, T. (2009). "A study on dynamic impact of vertical concrete cask tip-over using explicit finite element analysis procedures." *Annals of Nuclear Energy*, 36(2), pp. 213-221.

Kent, D.C., and Park, R. (1971). "Flexural Members with Confined Concrete." *Journal of the Structural Division.*, ASCE, Vol. 97, No ST7, pp. 1969-1990.

Kujawski, J. (1988). "Stable semi-explicit algorithms for non-linear dynamic problems." *Earthquake Engineering & Structural Dynamics*, 16(6), pp. 855-865.

Limberger, E., Brandes, K., & Herter, J. (1982). "Influence of mechanical properties of reinforcing steel on the ductility of reinforced concrete beams with respect to high strain rates." In Plauk, G. (Ed.). Concrete structures under impact and impulsive loading, p. 656. Germany

Lok, T. and Zhao, P. (2004). "Impact Response of Steel Fiber-Reinforced Concrete Using a Split Hopkinson Pressure Bar." *J. Mater. Civ. Eng.*, 16(1), pp. 54-59.

Malvar, L. (1998). "Review of Static and Dynamic Properties of Steel Reinforcing Bars." *ACI Materials Journal*, 95(5), pp. 609-616.

Menegotto, M., and Pinto, P.E. (1973). "Method of Analysis for Cyclically Loaded Reinforced Concrete Plane Frames Including Changes in Geometry and Nonelastic Behavior of Elements under Combined Normal Force and Bending." *IABSE Symposium on Resistance and Ultimate Deformability of Structures Acted on by Well-Defined Repeated Loads*, Final Report, Lisbon.

Miranda, I., Ferencz, R. and Hughes, T. (1989). "An improved implicit-explicit time integration method for structural dynamics." *Earthquake Engineering & Structural Dynamics*, 18(5), pp. 643-653.

Mullapudi, T. and Ayoub, A. (2010). "Modeling of the seismic behavior of shear-critical reinforced concrete columns." Engineering Structures, 32(11), pp. 3601-3615.

Neuenhofer, A. and Filippou, F. (1997). "Evaluation of Nonlinear Frame Finite-Element Models." Journal of Structural Engineering, 123(7), pp.958-966.

Pezeshk, S. and Camp, C. (1995). "An explicit time integration technique for dynamic analyses." *International Journal for Numerical Methods in Engineering*, 38(13), pp. 2265-2281.

Ross, C.A., Thompson, P.Y., Tedesco, J.W., (1989). "Split-hopkinson pressure-bar tests on concrete and mortar in tension and compression." ACI Mater. J. 86 (5), pp. 475–481.

Saatci, S. and Vecchio, F. (2009). "Effects of Shear Mechanisms on Impact Behavior of Reinforced Concrete Beams." ACI Structural Journal, 106(1).

Scott, B.D., Park, R., and Priestley, M.J.N. (1982). "Stress-Strain Behavior of Concrete Confined by Overlapping Hoops at Low and High Strain Rates." *ACI. Journal*, Vol. 79, pp. 13-27.

Spacone, E., Filippou, F. and Taucer, F. (1996). "Fibre beam-column model for non-linear analysis of r/c frames: part i. formulation." *Earthquake Engineering & Structural Dynamics*, 25(7), pp.711-725

Sun, J., Lee, K. and Lee, H. (2000). "Comparison of implicit and explicit finite element methods for dynamic problems." *Journal of Materials Processing Technology*, 105(1-2), pp.110-118.

Taylor, R. (2014). *FEAP - Finite Element Analysis Program*. Berkeley: University of California.

Tenek, L. (2015). "A Beam Finite Element Based on the Explicit Finite Element Method." *International Review of Civil Engineering (IRECE)*, 6(5), p. 124.

Yang, D., Jung, D., Song, I., Yoo, D. and Lee, J. (1995). "Comparative investigation into implicit, explicit, and iterative implicit/explicit schemes for the simulation of sheet-metal forming processes." Journal of Materials Processing Technology, 50(1-4), pp.39-53.

Yoshida, Y., Masuda, N., Morimoto, T. and Hirosawa, N. (1980). "An incremental formulation for computer analysis of space framed structures." *Journal of Structural Mechanics and Earthquake Engineering*, JSCE 300, pp. 21-32. (in Japanese)

LIST OF FIGURE CAPTIONS

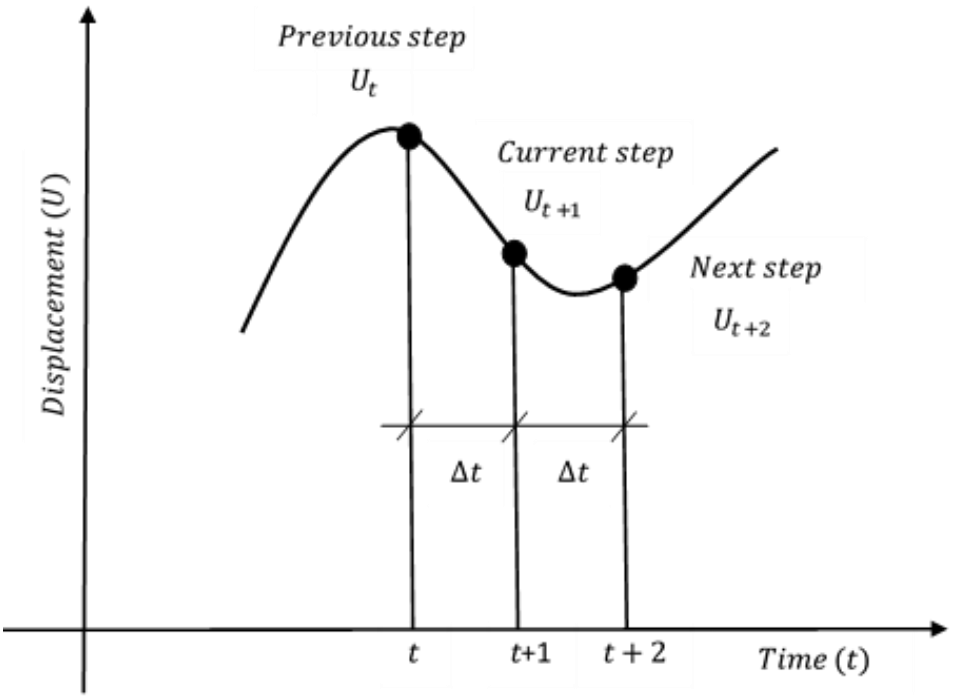

Fig. 1. Time integration graph.

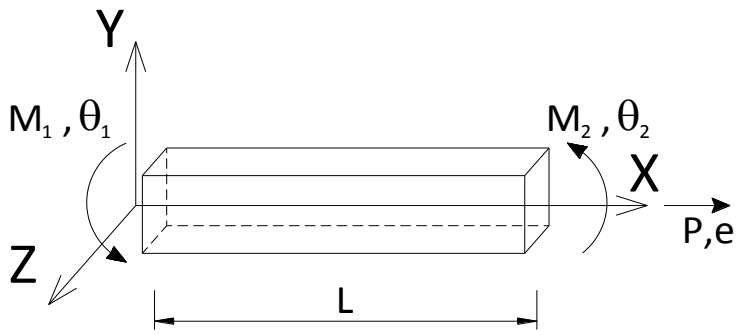

Fig. 2. Element nodal forces and degrees of freedom in the corotational frame.

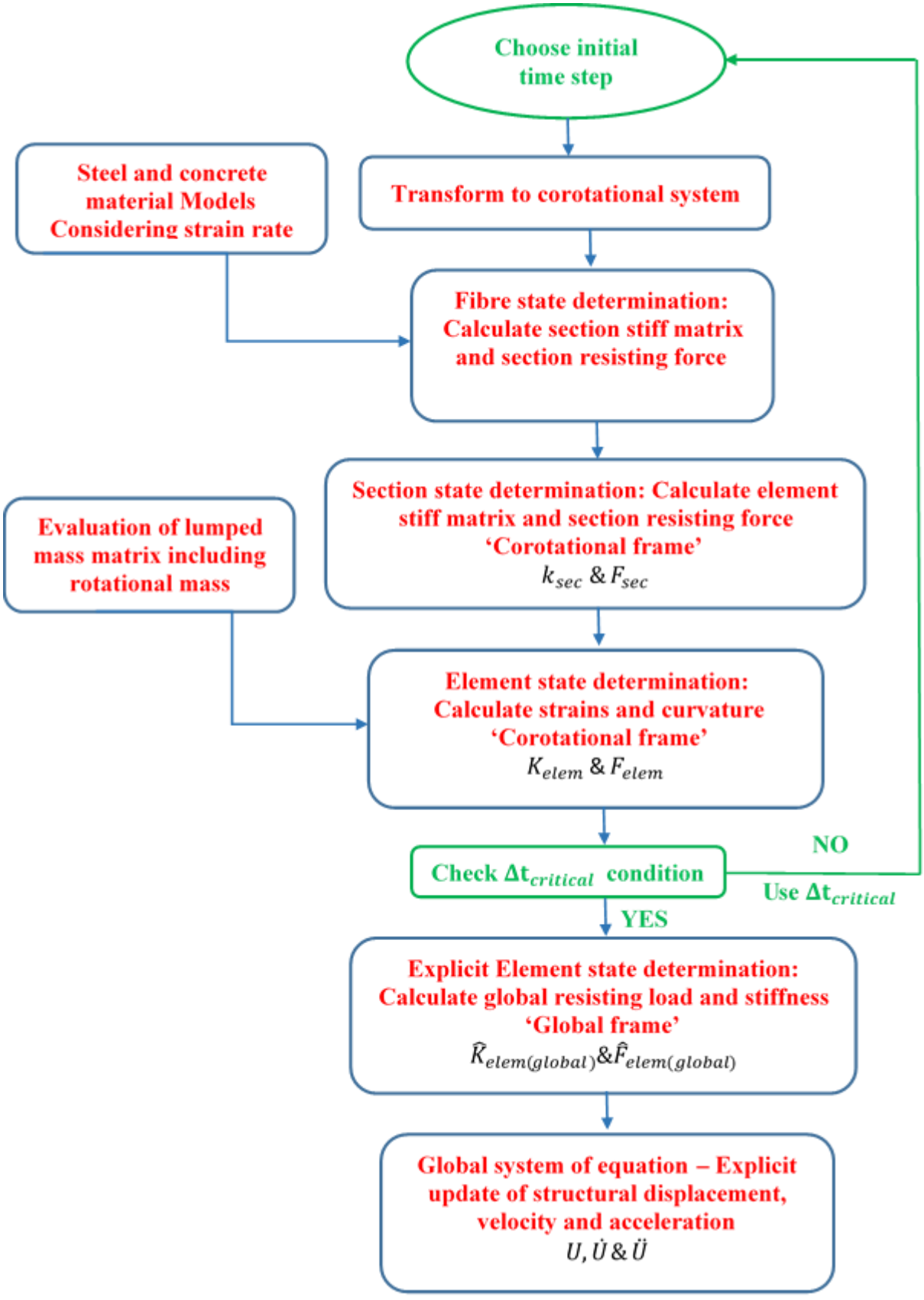

Fig. 3. Flowchart diagram of the proposed explicit fiber beam elements.

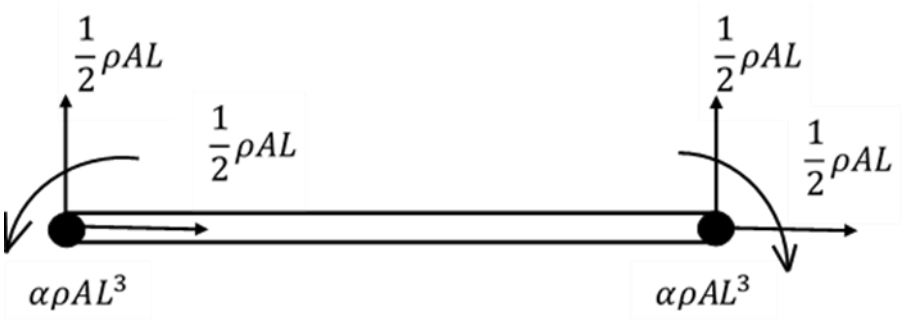

Fig. 4. Direct mass lumping for two-node plane beam element.

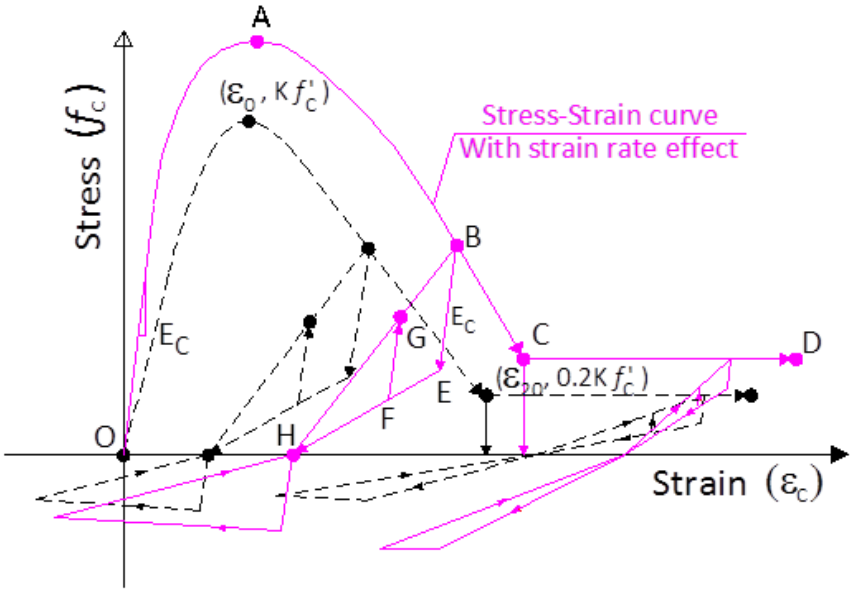

Fig. 5. Concrete material model with and without strain rate effect.

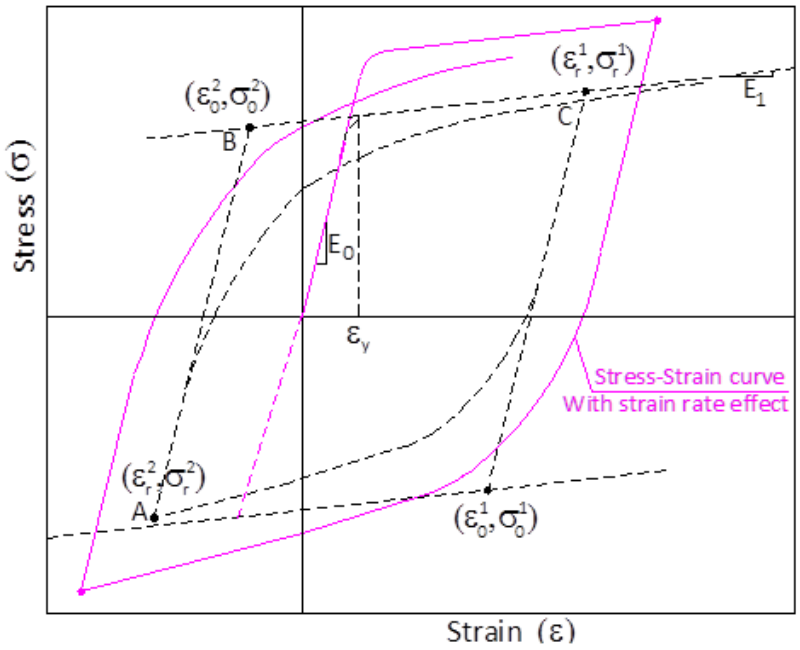

Fig. 6. Menegotto-Pinto Cyclic stress-strain curve of mild steel bar with and without strain rate effect.

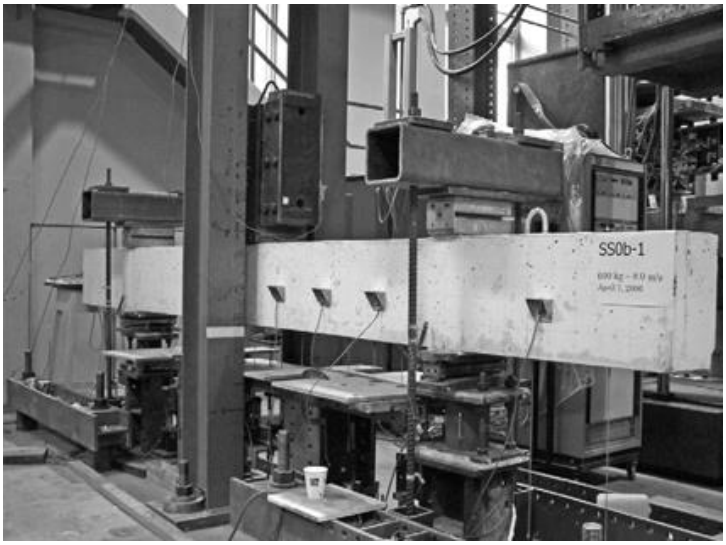

Fig. 7. Test setup of the beams, figure from **(Saatci and Vecchio 2009)**.

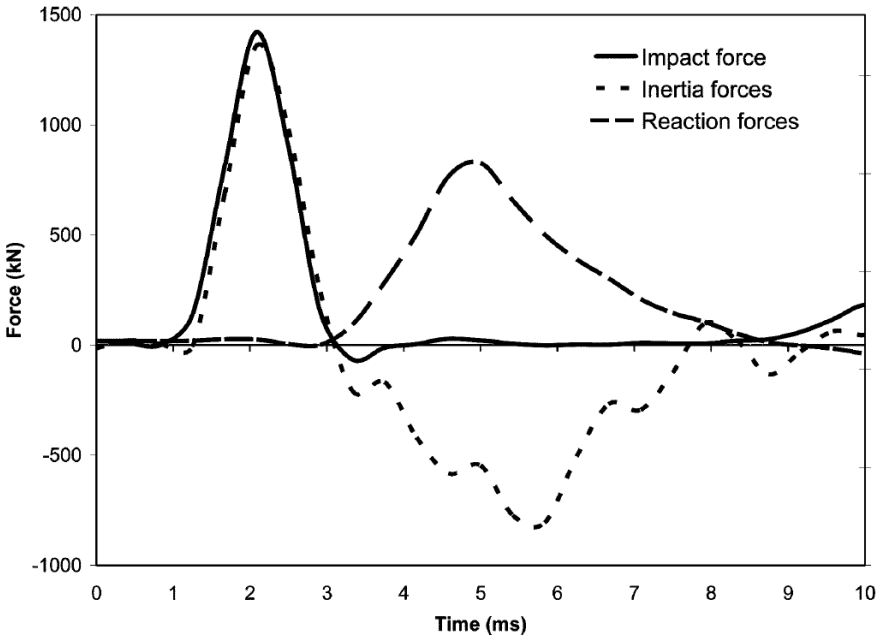

Fig. 8. Impact and reaction forces vs time for sample SS3a-1, figure from **(Saatci and Vecchio 2009)**.

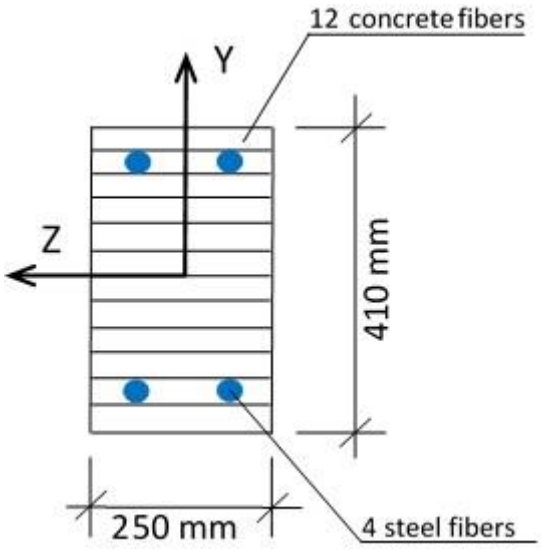

Fig. 9. Fiber beam element cross section mesh for sample SS3a-1.

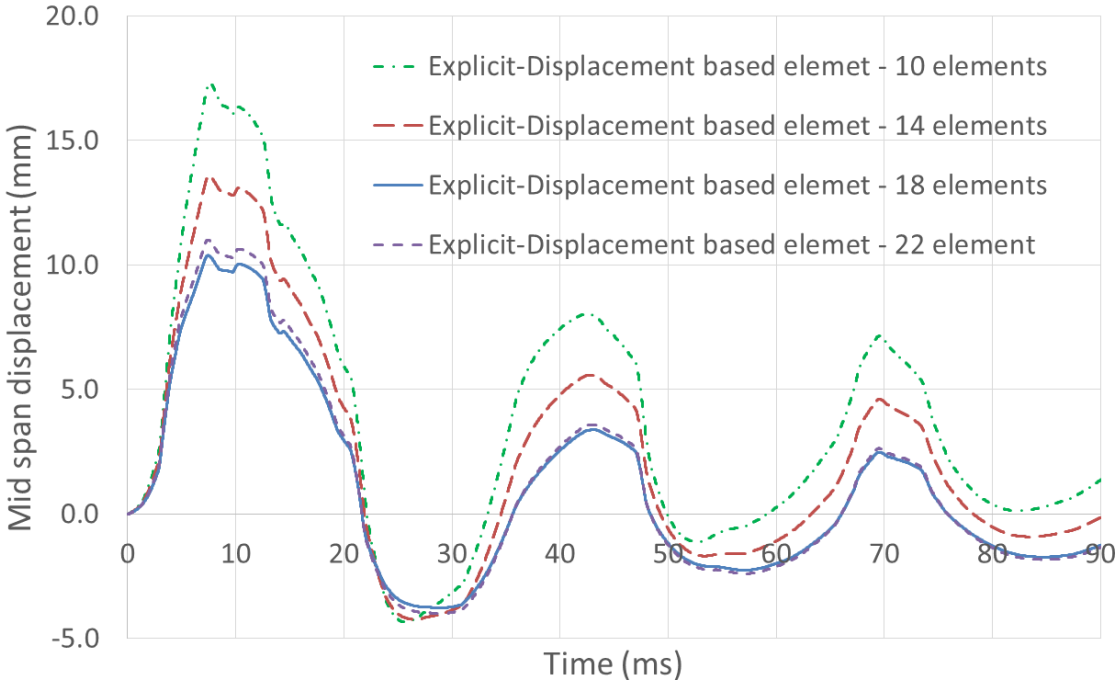

Fig. 10. Conversion study for the explicit displacement base element using sample SS3a-1.

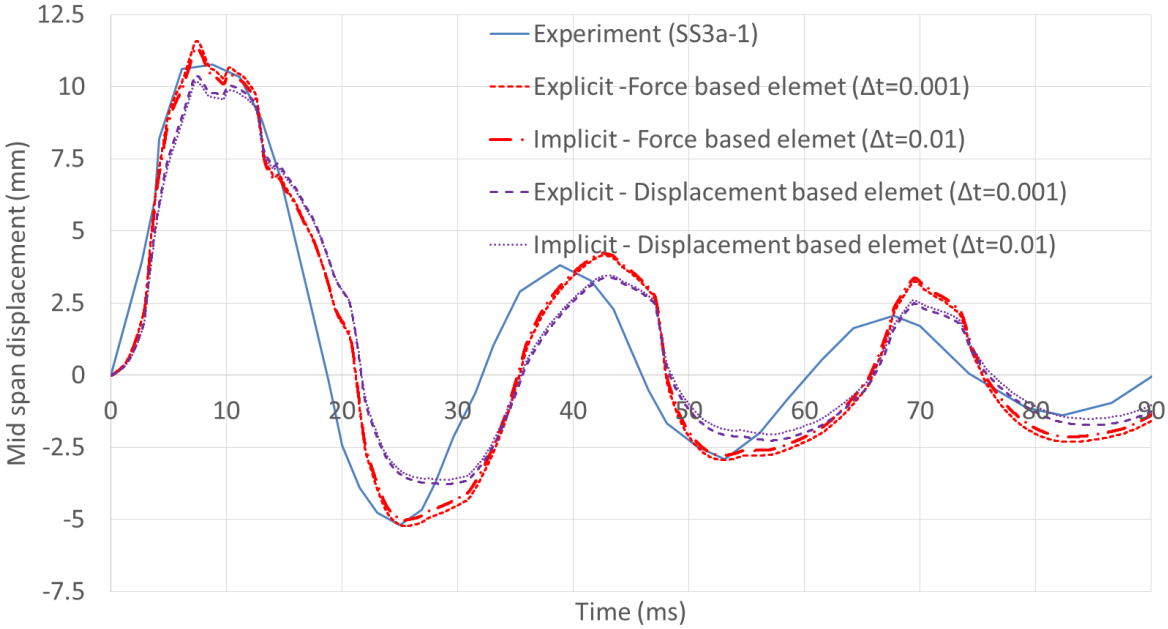

Fig. 11. Midpoint displacement time history of sample SS3a-1.

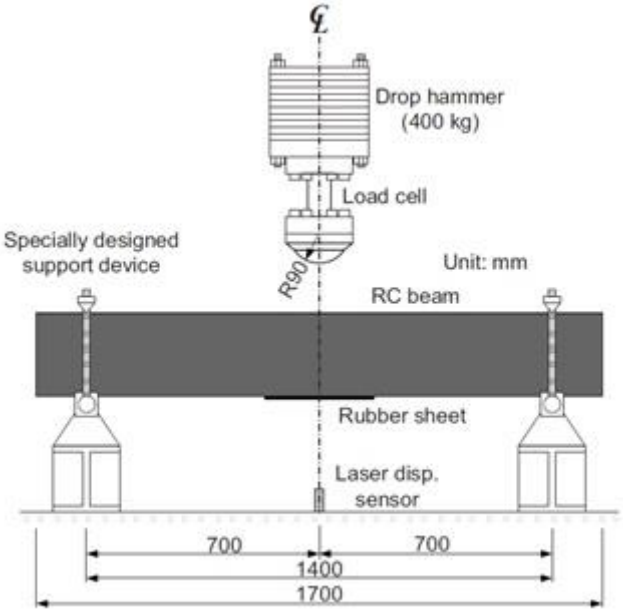

Fig. 12. Drop hammer impact test setup, figure from **(Fujikake et al. 2009)**.

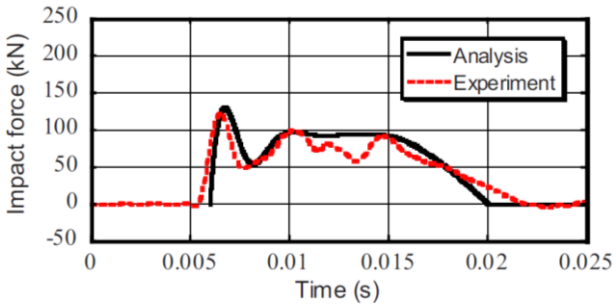

Fig. 13. Impact load history for sample S1616-A, figure from **(Fujikake et al. 2009)**.

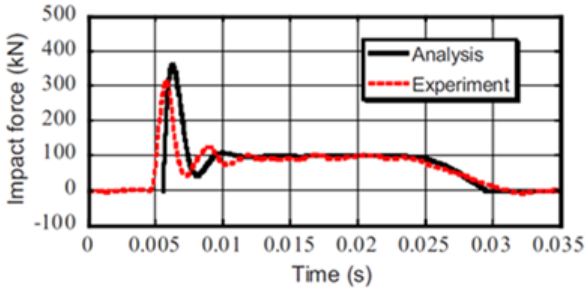

Fig. 14. Impact load history for sample S1616-D, figure from **(Fujikake et al. 2009)**.

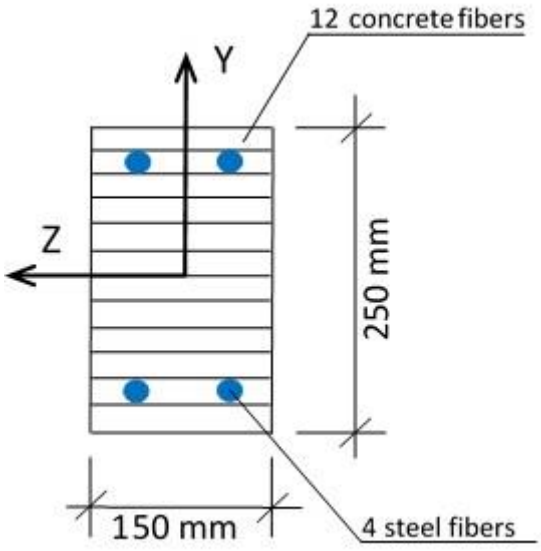

Fig. 15. Fiber beam element cross section mesh for sample S1616-A and S1616-D.

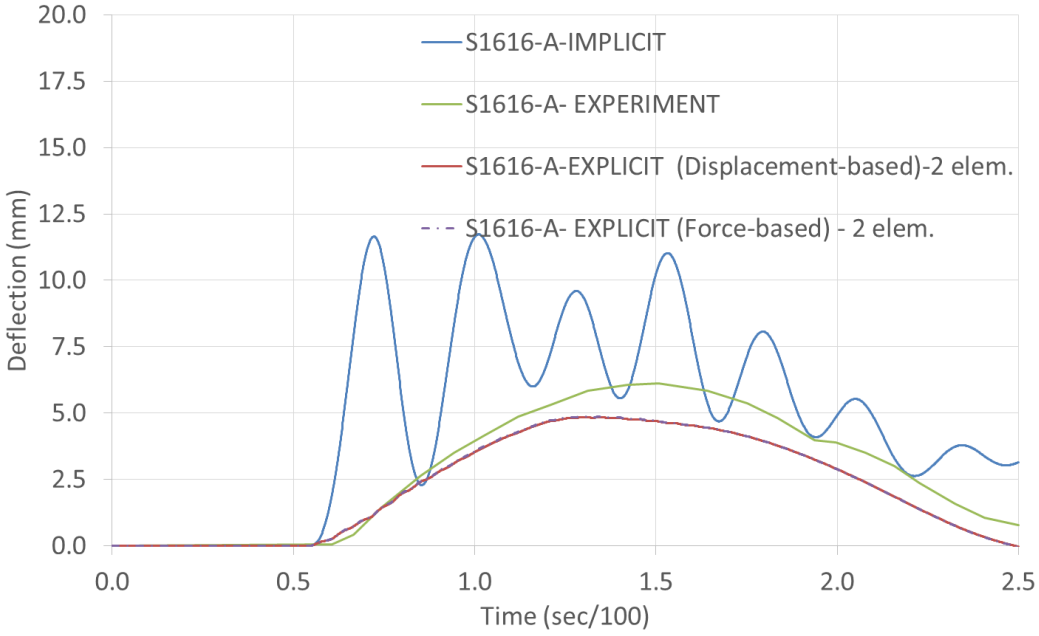

Fig. 16. Deflection time history for specimen S1616-A.

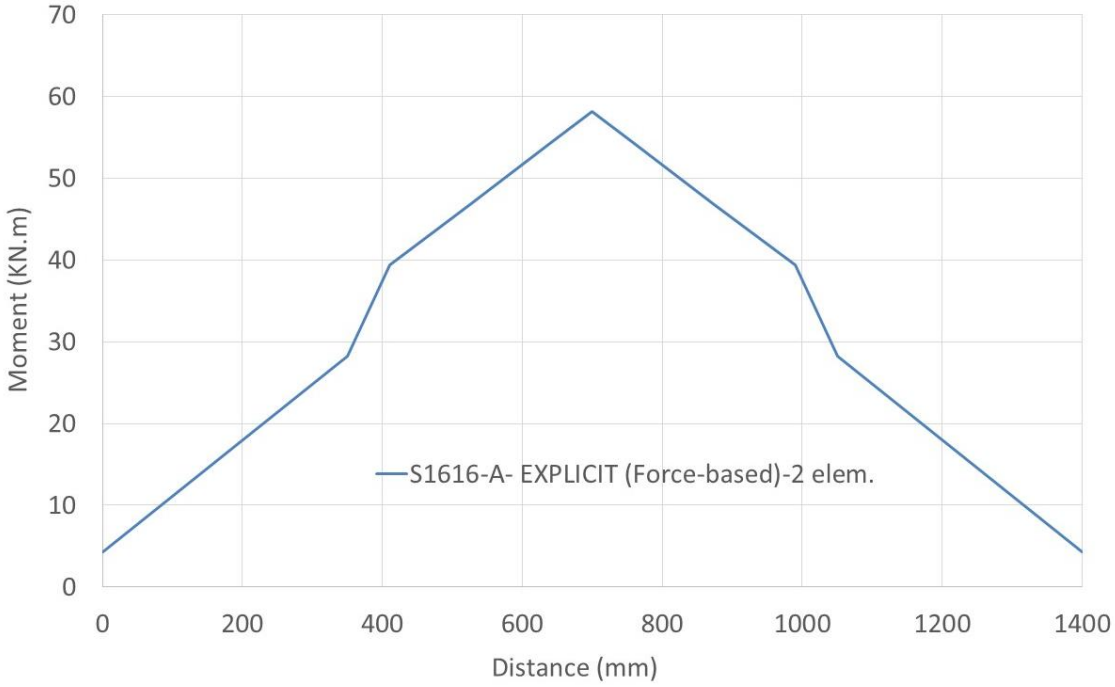

Fig.17. Bending moment at maximum displacement using the explicit force based element (specimen S1616-A).

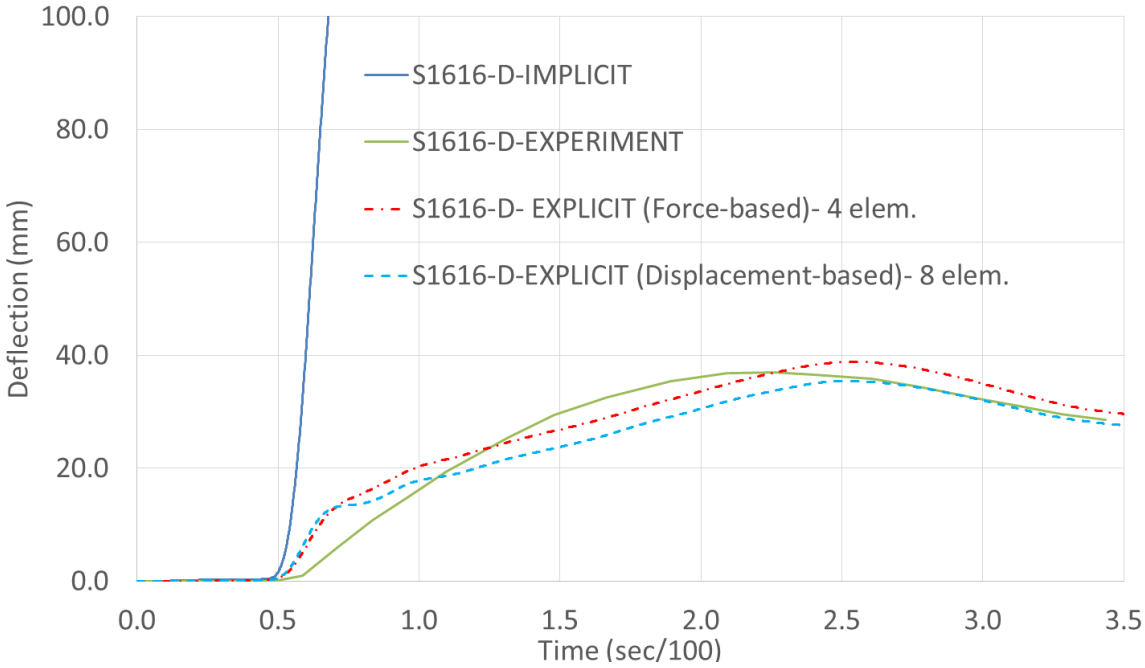

Fig. 18. Deflection time history for specimen S1616-D.

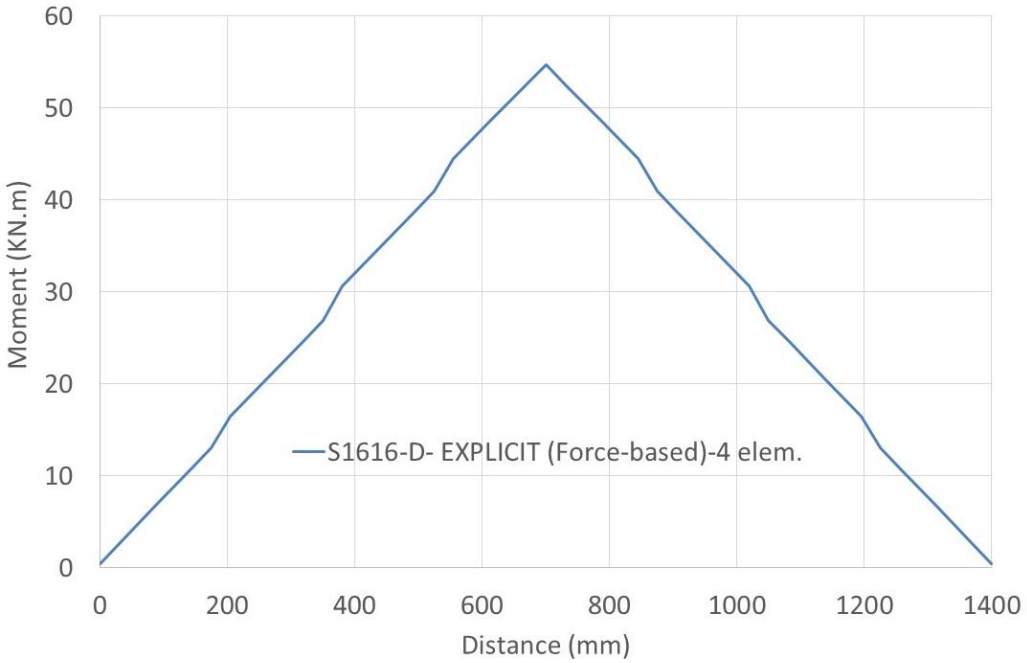

Fig.19. Bending moment at maximum displacement using the explicit force based element (specimen S1616-D).